Optical properties of CdS:Pb thin layer deposited on glass substrate

Hariom Kumar Kaushik[a], Sushil Kumar[b*], Megha Gupta Chaudhary[b] & Savidh Khan[c]

[a]Mahamana Malviya Degree College, Khekra, Baghpat 250 101, India

[b]SRM University, NCR Campus, Modinagar 201 204, India

[c]School of Physics and Materials Science, Thapar Institute of Engineering and Technology, Patiala 147 004, India

The thermal evaporation technique has been used to deposit a polycrystalline cadmium lead sulphide thin film ($Cd_{1-x} Pb_xS$ with X=0.20) in a vacuum of about 10^{-5} Torr at 450 °C. This $Cd_{1-x} Pb_xS$ thin film has been investigated by X-ray diffraction technique. Optical constant like extinction coefficient (K), dielectric constant (€), and refractive index (n) have been measured from transmission spectrum in wavelength range from 700 nm to 1700 nm by manifacier's envelope method. Crystallite size estimated from the Scherrer method has been found to be 31.25 nm. Coefficient of absorption (α) as well as film thickness (t) has been estimated by means of transmission spectra. The lattice parameter (a), dislocation density (δ), inter planner spacing (d), and micro strain (ε) have been calculated. X-ray study reveals that film stoichiometry is maintained in deposited film. The optical study confirms that optical band gap of $Cd_{1-x} Pb_xS$ film can be tuned from visible to near infrared region (2.42-1.20 eV) using relatively low cost technique. The red shift in optical band gap has been observed for $Cd_{1-x} Pb_xS$ thin film. Pb doping increase absorbance in visible region and near infrared region compared to undoped CdS film. The large decrease in band gap has been observed which makes the film much suitable for absorbing layer in solar cells, IR detector and other photovoltaic and optoelectronic applications. In film band, gap of 1.13 eV has been achieved which shows that doping of Pb in CdS makes it suitable material for solar cell absorber and IR detectors. The film shows high transmittance (about 70 %) in near infrared region. The film is polycrystalline and highly stoichiometric.

Keywords: CdPbS thin film, XRD, Bandgap, Dielectric constant, Thermal evaporation technique

1 Introduction

Metal chalcogenides, sulphides, tellurides and selenides have been widely studied due to their optoelectronic applications such as solar cells, photo detectors thin films transistors[1-5] etc. The II-VI group semiconductors like CdS, ZnSe and ZnS have been extensively used for different applications like solar cells, piezoelectric transducers, LED, photo detectors and transparent UV protection devices[6-8].

There are three major solar cells technologies named as copper indium gallium selenide, amorphous silicon and cadmium telluride. Among above three technologies, CdTe solar cells are recently found to be the most efficient and cheaper than the others. Currently, the efficiency of CdTe solar cell is reported (20 %) which is indeed much greater than the efficiency of amorphous silicon solar cells[4] (12 %). Cadmium sulphide (CdS) serves as better hetero-structure with CdTe film. The CdS/CdTe hetero-structure has been drawn attention of researcher for better future of solar cell technology[9,10].

Cadmium sulphide (CdS) with band gap of 2.42 eV is commonly used as polycrystalline semiconductor thin films in electronic and optoelectronic devices such as solar cell, thin film transistor, light emitting diodes[8] etc. In order to use $Cd_{1-x} Pb_xS$ thin film as absorber layer in solar cell the deposited film required high absorbency in visible region[9,11]. To solve such problems doping of different elements like Al, Fe, Cu, In, Co, Mn, Ni, Zn, Te has been observed[12]. A large number of studies have already been done concerned to doping a CdS semiconductor for photovoltaic devices, infrared detectors and optoelectronic applications but it is still an open subject. The main focus of our present study is to discuss the absorbency of Pb doped CdS thin film for solar cell applications, infrared detectors and other photovoltaic and optoelectronic devices.

Hone *et al.* prepared $PbS_{1-x}Se_x$ thin film by chemical bath deposition which shows good absorbency and tailoring of optical band gap of PbS_1-xSe_x thin films down to visible region[11].

Ma *et al.* prepared Te doped CdS thin films by vacuum technique which indicates that in visible

---

*Corresponding author (E-mail: drskbhargava2011@gmail.com)

region transmittance decreases at relatively low Te amount which is undesirable for window layers[12]. Sivaraman *et al.* prepared chlorine doped thin films by spray deposition technique. The transmittance of Cl-doped CdS thin films increases significantly as chlorine concentration is increased[13].

Narasimman *et al.* prepared Zr-doped CdS film by spray method which shows that Zr-doping helps in increasing transparency in visible region[14].

In present work, $Cd_{1-x} Pb_x S$ (with X=0.20) ternary thin film is deposited by thermal evaporation technique at glass substrate. Compare to other recent technologies, the thermal evaporation method is an advantage of relatively low cost[4]. Since, deposition techniques also play an important role in better thin film preparation. Here in order to discuss absorbency, transparency and other properties we have utilized thermal evaporation method to prepare Pb-doped CdS thin film. Effect of doping on optical and structural properties is investigated.

2 Experimental Details

The thin film of $Cd_{1-x} Pb_x S$ (with X=0.20) was deposited by thermal evaporation technique. The stoichiometric amount of CdS & PbS compounds of high purity (Sigma Aldrich, purity=99.999 %) were used to prepare above mention composition. This $Cd_{1-x} Pb_x S$ powder was used as evaporation source material. This powder alloy is placed in molybdenum boat filament within a high vacuum chamber having pressure of about 2×10^{-5} torr. To get film uniformity and to avoid texturing effect substrate and filament distance is kept about 10 cm. To check crystalline phase of film deposited we have utilized X-ray diffraction technique using CuK_α radiation λ=1.5418 Å. Since optical characterization is essential for photovoltaic as well as sensor applications so samples were scrutinized by using UV-visible-NIR spectrophotometer (Varian Carry 5000). The film deposited at 450 °C has found the thickness of approximately 3.80 micrometer.

3 Results and Discussion

Typical X-ray diffraction diagram of $Cd_{1-x} Pb_x S$ thin film is displayed in the Fig. 1 with (220) peak at 2Θ =43.34°. The observed peak can be attributed to lattice planes of stable cubic phase. The main peak in XRD pattern of $Cd_{1-x}Pb_x S$ indicates the addition of Pb ions into the CdS lattice. This shows polycrystalline nature of the film.

The crystallite size (t) of the prepared $Cd_{1-x} Pb_x S$ (with X=0.20) thin film is obtained by the Scherrer's formula[15] as follows:

$$t = 0.94\lambda/\beta Cos\,\theta \cdot \qquad ...(1)$$

where, λ is the wavelength of X-ray in nm, β is the full width by half maximum of the diffraction peak in radian and θ is the Bragg's angle of given peak. Estimated value of crystallite size is about 31.25 nm.

Other parameters such as inter planner distances ($d_{h\,k\,l}$), the dislocation density (δ) and micro strain (ε) were calculated for (220) plane of $Cd_{1-x} Pb_x S$ using following formulas:

$$\delta = 1/D^2 \qquad ...(2)$$

$$4\varepsilon = \beta\,Cos\,\theta \qquad ...(3)$$

$$d = a/\sqrt{(h^2 + k^2 + l^2)} \qquad ...(4)$$

The lattice parameter value for cubic lattice is calculated by following formula:

$$a = \lambda\,\sqrt{(h^2 + k^2 + l^2)}/2sin\theta \qquad ...(5)$$

The lattice parameter (a), dislocation density (δ), inter-planner spacing (d), and micro strain (ε) were calculated as 5.83 Å, 1.02 lines/m³, 2.06 Å and 0.1159, respectively.

3.1 Optical characterization

The optical transmittance measurement was carried out by UV-visible-NIR spectrophotometer. Figure 2 shows transmittance versus wavelength of $Cd_{1-x} Pb_x S$ (with x=0.2) thin film exhibited higher transmittance (about 70 %) in NIR region. The higher transmittance in NIR region is required in order to utilize maximum sun light for photovoltaic and optoelectronic applications. Increase or decrease in transmittance could be due to the presence of defects, large surface roughness and grain boundary scattering[16-18].
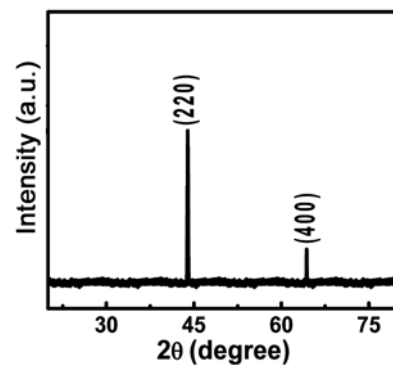

Fig. 1 — X-ray diffraction pattern of $Cd_{1-x} Pb_x S$ (with X=0.20) thin film.
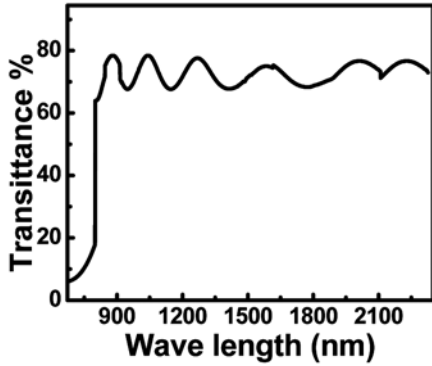
Fig. 2 — UV-visible-IR spectra of $Cd_{1-x}Pb_xS$ (with x=0.20) thin film.

Optical band gap is one of the essential parameter of semiconductor thin films. Tauc's plot is used to estimate the optical band gap of $Cd_{1-x}Pb_xS$ (with x=0.2) thin film.

$$(\alpha h\nu) = (h\nu - E_g)^r \qquad \ldots (6)$$

where, $h\nu$ is the photon energy, α is the absorption coefficient[23]. The exponent 'r' governs by the transition, where=1/2, 2, 3/2 and 3 for allowed direct, allowed indirect, forbidden direct and forbidden indirect transition, respectively. Figure 3 shows the plot of $(\alpha h\nu)^2$ versus (hν) for $Cd_{1-x}Pb_xS$ thin film and the obtained band gap value lies in the semi-conductor range (1.13 eV).

It is well-known fact that semiconductors having band gap in the range of 1-1.5 eV, resulting suitable for obtaining high energy conversion efficiency (about 30 %) when utilized as an absorber material in solar cell applications. The band gap decreases with the doping of Pb in place of Cds. The decrease in band gap confirms the formation of ternary Cd-PbS thin film with strong quantum confinement. This decrement in band gap might be due to formation of impurity and defects. The optical parameters were figured out with the help of 'envelope method' of Manifacier *et al.*[19].

Extinction coefficient and refractive index variation with increasing wavelength (900-1800) of the prepared film was studied by the following relation.

Deposited film's refractive index (n) is given by:

$$n = \sqrt{\sqrt{N^2 - n_o^2 n_1^2} + N} \qquad \ldots (7)$$

$$N = \left(\frac{n_0^2 + n_1^2}{2}\right) + 2n_0 n_1 \left[\frac{1}{T_{min}} - \frac{1}{T_{max}}\right] \qquad \ldots (8)$$
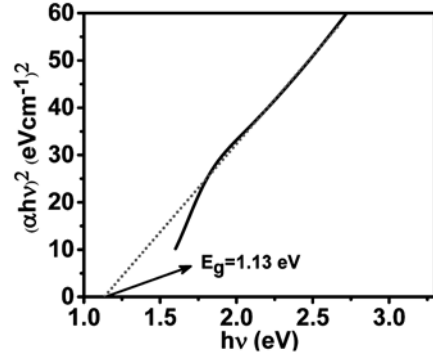

Fig. 3 — Tauc plot $((\alpha h\nu)^2$ versus hν) of $Cd_{1-x}Pb_xS$ (with x=0.20) thin film showing optical band gap.
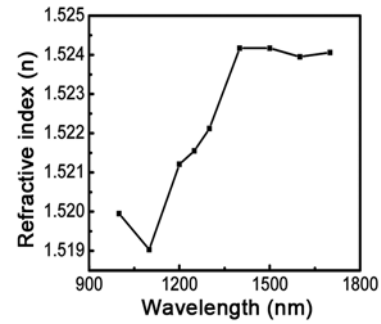

Fig. 4 — Refractive index as a function of wavelength $Cd_{1-x}Pb_xS$ (with x=0.2) thin film.

Extinction coefficient (k) was determined from following results:

$$K = \left[-\frac{\lambda}{4\pi t}\right] \ln P' \qquad \ldots (9)$$

Where,

$$P' = \frac{C_1\left[1 - \left(\frac{T_{max}}{T_{min}}\right)^{\frac{1}{2}}\right]}{C_2\left[1 + \left(\frac{T_{max}}{T_{min}}\right)^{\frac{1}{2}}\right]}$$

and $C_1 = \{n + n_o\}\{n_1 + n\}$,

$$C_2 = \{n - n_o\}\{n_1 - n\}$$

The change in refractive index (n) and extinction coefficient (k) with wavelength are shown in the Figs 4 and 5, respectively. It has been observed that both the refractive index as well as the extinction coefficient of the film is increased as wavelength increases. An increase in extinction coefficient
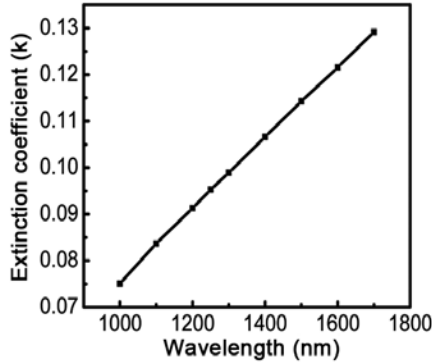
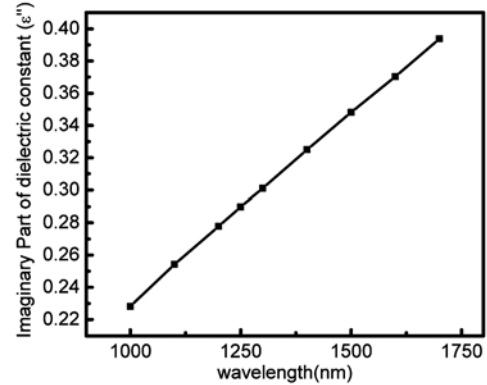Fig. 5 — Extinction coefficient as a function of wavelength for $Cd_{1-x}Pb_xS$ thin film (with x=0.2).

Fig. 7 — Imaginary part of dielectric constant as a function of wavelength of $Cd_{1-x}Pb_xS$ (with x=0.20).

indices of refraction. The average thickness of the film was estimated at 3.80 micrometer.

4 Conclusions

In the present work, $Cd_{1-x}Pb_xS$ (with X=0.20) thin film with average thickness of 3.80 micrometer has been prepared successfully by physical vapor deposition technique. The optical band gap decreases with the doping of Pb in CdS. The increase in the absorption properties of thin film is confirmed as extinction coefficient improved by the doping. The refractive index, extinction coefficient, dielectric constants and dielectric loss were evaluated by transmission spectra and found to increase as frequency increases. Surface morphology and grain size are discussed by analyzing the XRD pattern. The fine crystallite size (31.25 nm) is achieved which is required to improve strength and toughness of the film. The optical propertied can be tuned with Pb doping and film can utilized for various optoelectronic and photovoltaic devices. Ultrahigh vacuum is required for the further improvement in the film. Single crystalline thin film can be obtained by controlling the deposition conditions.
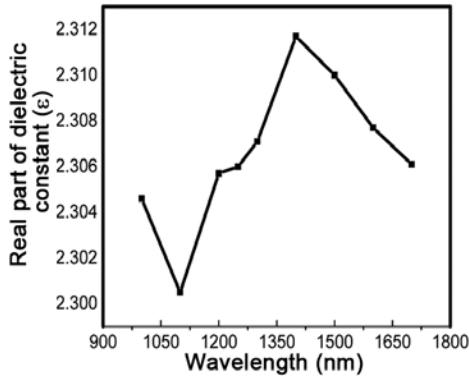

Fig. 6 — Real part of dielectric constant as a function of wavelength of $Cd_{1-x}Pb_xS$ (with x=0.2)

suggests the light absorption in sufficient range of visible and infrared region for $Cd_{1-x}Pb_xS$ (with x=0.2) thin film.

Real part (dielectric constant, ε') and imaginary part (dielectric loss, ε") of prepared film was measured using the following relations:

$$\varepsilon' = n^2 - k^2 \qquad \qquad ... (10)$$

$$\varepsilon'' = 2nk \qquad \qquad ... (11)$$

The change in dielectric constant and dielectric loss with respect to frequency is shown in Figs 6 and 7. The dielectric constant exhibits non-linear trend with frequency, whereas dielectric loss shows linear trend with respect to frequency.

The film thickness was estimated using following relation[20-22]:

$$t' = [M \lambda_1 \lambda_2]/ 2[n(\lambda_1) \lambda_2 - n(\lambda_2) \lambda_1] \qquad ... (12)$$

M is the number of vibrations between two maxima (M=1 between two successive minima or maxima). λ_1, $n(\lambda_1)$, λ_2, $n(\lambda_2)$ are the corresponding wavelength and

References

1 Abza T, Ampong F K, Hone F G, Nkum R K & Boakye F, *Thin Solid Films*, 666 (2018) 28.

2 Barman B, Bangera K V & Shivakumar G K, *Superlatt Microsturt*, 123 (2018) 374.

3 Moraa M B, Sarria O A, Monroy B M , Péreze C D H & Lugo J E, *Sol Energy Mater Sol C*, 165 (2017) 59.

4 Nykyruy L I, Yavorskyi R S, Zapukhlyak Z R, Wisz G & Potera P, *Opt Mater*, 92 (2019) 319.

5 Han G, Zhang S, Boix P P, Wong H L, Sun L & Lien S Y, *Prog Mater Sci*, 87 (2017) 246.

6 Perez R M, Hernandez J S, Puente G & Galan O V, *Sol Energy Mater Sol C*, 8 (2009) 79.

7 Thanikaikarasan S, Mahalingam T, Raja M & Velumani S, *Mater Sci Semicond Proc*, 37 (2015) 215.

8 Moualkia H, Hariech S & Aida M S, *Thin Solid Films,* 518 (2009) 1259.

9 Dawood Y Z*, Energy Proc*, 119 (2017) 536.

10 Lee T D & Ebong A U, *Renew Sustain Energy Rev*, 70 (2017) 1286.

11 Hone F G, Ampong F K, Nkum R K & Boakye F*, J Mater Sci: Mater Electron*, 28 (2017) 2893.

12 Wei Z, Wang Y, Ma L & Wu X S, *Physica B*, 525 (2017) 98.

13 Sivaraman T, Narasimman V, Nagarethinam V S & Balu A R, *Prog Nat Sci-Mater*, 25 (2015) 392.

14 Narasimman V, Nagarethinam V S, Usharani K & Balu A R, *Optik*, 138 (2017) 398.

15 Cullity B D, *Elements of X-ray Diffraction*, (Addison-Wesley Publication Comp), 1956.

16 Kumar P, Kumar P, Kumar A, Meena R C, Tomar R, Chand F & Asoken K, *J Alloys Compd*, 672 (2016) 543.

17 Sugumaran S, Ballen C S & Bheeman D*, Opt Mater* 72, (2017) 618.

18 Zaki A A & El-Amin A A, *Opt Laser Technol,* 97 (2017) 71.

19 Manifacier J C, Gasiot J & Fillard J P, *J Phys E*, 9 (1976) 1002.

20 Swanepoel R, *J Phys E: Sci Instrum*, 17 (1984) 896.

21 Kumar S & Sharma S D, *J Pure Appl Sci Technol,* (2014) 5.

22 Kumar S, Kaushik H K & Sharma S D, *Int J Educat Sci Res Rev*, 4 (2017) 10.

23 Yang E S*, Fundamental of Semiconductor Devices* (McGraw–Hill, New York), 1978.